



Sol-Gel Derived Blue-Emitting SrAlO:Mn,Dy Nano-Phosphors

KEYWORDS

G. Suresh

V.T. Jisha

Department of Engineering Physics, FEAT, Annamalai University, Chidambaram 608 002. Tamilnadu, India.

Christian College, Kattakada, Thiruvananthapuram, 695572. India.

ABSTRACT Blue-emitting divalent Dy, Mn activated strontium aluminate (SrAlO :Mn,Dy) phosphor were synthesized by Sol-Gel method using Strontium Acetate, Aluminum Nitrate as raw material and 2-methoxyethanol as complexing agent. The morphology, composition and structure were characterized by scanning electron microscopy (SEM), energy dispersive X-ray (EDS) and X-ray diffraction (XRD) respectively. The nanomaterials emit blue luminescence with a peak wavelength at 402 nm and 460 nm under near-ultraviolet excitation at 360 nm. The Dy and Mn doping can decrease the amount of defects, which leads to the suppression of luminescence intensity.

Introduction

Luminescent semiconductor nano-crystals, have attracted great deal of attention in the past few decades due to their technological importance to improve their luminescent properties and to meet the requirement of different display and luminescence devices. In particular rare earth doped aluminates [1-7] serve as an important class of phosphors for fluorescent lamp and phosphorescence applications. Among these phosphors, strontium aluminates phosphors doped with rare-earth metal ions have emerged as materials with great potential. The doping ions act as recombination centers for the excited electron-hole pairs and result in strong and characteristic luminescence. In doped compound semiconductors, in contrast to the undoped semiconductors, the impurity states can play a special role in affecting the electronic energy structures and transition probabilities [8-10]. The strontium aluminate phosphors such as SrAl₂O₄ [11-19] tend to give blue or green long afterglow emission. It is believed that when the ratio of Al/Sr is equal to 2, an emission peak lies at about 520 nm [20], and when the ratio is above 2, a blue emission peak at approximately 495 nm appears [21].

In this work, we report the preparation and characterization of SrAlO and Mn, Dy doped SrAlO nanoparticle via Sol Gels method. The effect of the Mn, Dy doping on the photoluminescence of SrAlO, the morphology, and the structural properties were investigated.

Experiment

The SrAlO and Mn, Dy doped SrAlO nanoparticles were prepared by the sol-gel method. All the reagents used in the experiments were in analytical grade and used without any further purification. 80% of 2M Strontium acetate [(CH₃COO)₂ Sr.2H₂O, >98.5%] with 10% of Aluminum acetate [C₄H₆AlO₄.4H₂O, >99.0%] and 10% of Manganese acetate for SrAl₂O₄:Mn and 10% of Dysprosium Nitrate for SrAl₂O₄:Dy were used as the precursors. In a typical procedure, Stoichiometric mixtures of Strontium acetate and Aluminum acetate dissolved in 2-methoxy ethanol. The solutions were mixed on a magnetic stirrer at 80°C. After sometime a fixed amount of ammonia was added to the above mixture drop wise to maintaining pH values around 10 with continuous stirring and heating. During the reaction, it was noticed that the solution became viscous (con-

verting to gel). On further heating, white ash colour powder was obtained. The synthesized powder was annealing at 900°C for 2 hour. Dysprosium and manganese was doped by adding Dysprosium nitrate and manganese nitrate into at 10%.

Result and Discussion

The structure and phase purity of the SrAlO and SrAlO:Mn, Dy phosphor were investigated by XRD. The XRD patterns were obtained. Results are shown in Fig. 1(a-c) for the SrAlO and Mn, Dy doped SrAlO. All diffraction patterns were obtained using CuK α radiation ($\lambda = 1.54051 \text{ \AA}$), at 30 kV and 15 mA. Measurements were made from $2\theta = 10^\circ$ to 80° with steps of 0.02° . The XRD patterns of the powders revealed that the structure of SrAlO is monoclinic, which is match with JCPDS data card No.25-1208. No diffraction peaks of Mn, Dy or other impurities phases are detected in our samples, indicating that Mn, Dy ions would uniformly substitute into the Sr sites or interstitial sites in SrAlO lattice

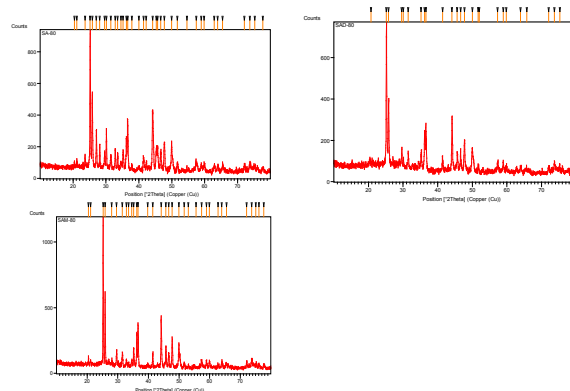


Fig.1(a-c). XRD patterns of (a) SrAlO (b) SrAlO:Dy and (c) SrAlO:Mn

Fig.1(a-c). XRD patterns of (a) SrAlO (b) SrAlO:Dy and (c) SrAlO:Mn

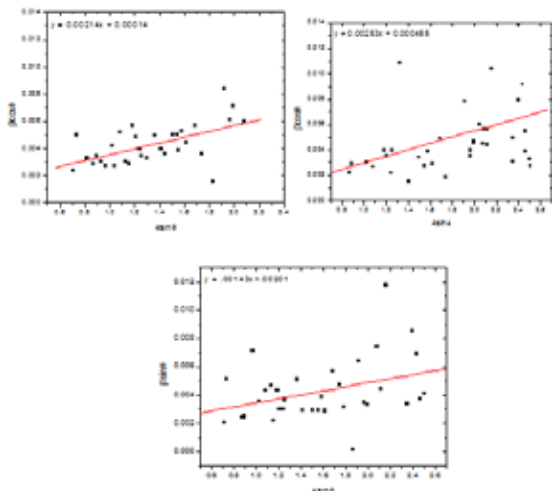


Fig.2(a-c). The Hall-Williamson plots for (a) SrAlO (b) SrAlO:Dy and (c) SrAlO:Mn

Williamson–Hall equation is used to calculate the strain and particle size of the samples. The Williamson–Hall equation is expressed as follows:

$$\beta \cos \theta = \frac{k\lambda}{D} + 4\epsilon \sin \theta$$

In this equation, $\beta \cos \theta$ is plotted against $4 \sin \theta$. Using a linear extrapolation to this plot, the intercept gives the particle size $k\lambda/D$ and the slope represents the strain (ϵ) for SrAlO and SrAlO:Mn,Dy nanoparticles as shown in Figure 2(a-c). The internal lattice strain value was found to be 0.0001 0.00045 and .002 for, SrAlO and SrAlO:Mn,Dy respectively. Using Williamson–Hal method, the mean grain sizes are evaluated, which are 64.7, 53.7 and 96.9 nm for the nanoparticles SrAlO, SrAlO:Dy and SrAlO:Mn.

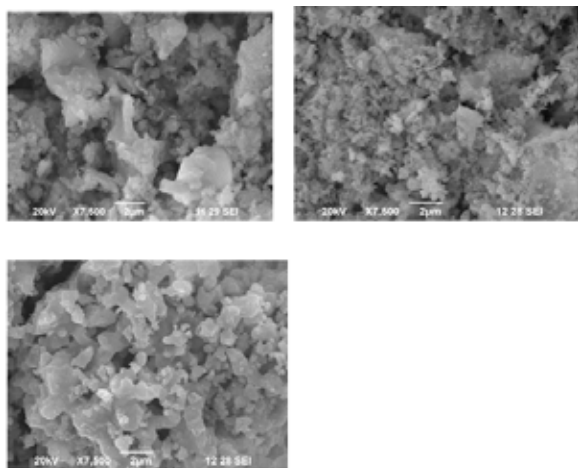


Figure 3. SEM images (a) SrAlO (b) SrAlO:Dy and (c) SrAlO:Mn

SEM was used to study the surface morphology of the films. A representative micrograph of the film is shown in Fig. 3(a-c). The micrograph also showed that the particles

were interlinked with each other, leading to the formation of big crystals. Also, it is found that some irregular aggregations formed in the sample. . The grains are multi-sized with number of distinct micro-structural. In case of the doped sample SEM shows different morphological structure. The presence of bigger particles is attributed to the growth of small particles, which is a result of the sol–gel synthesis.

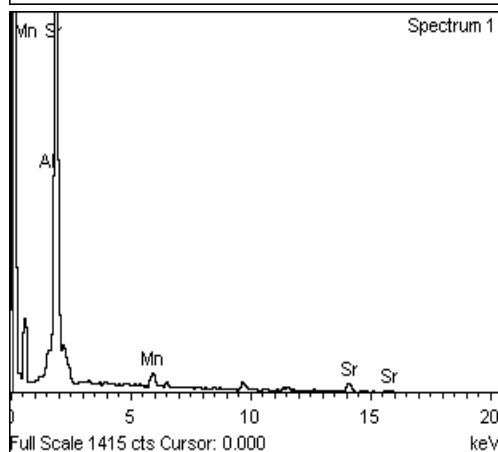
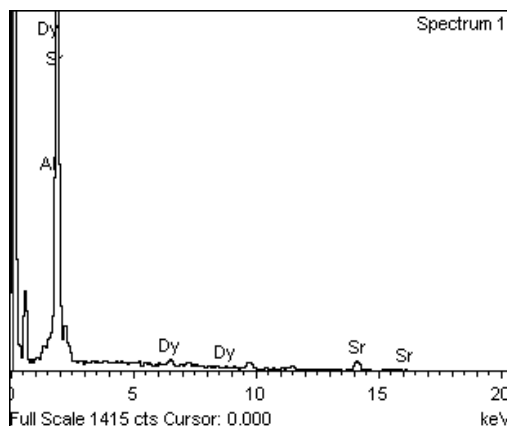
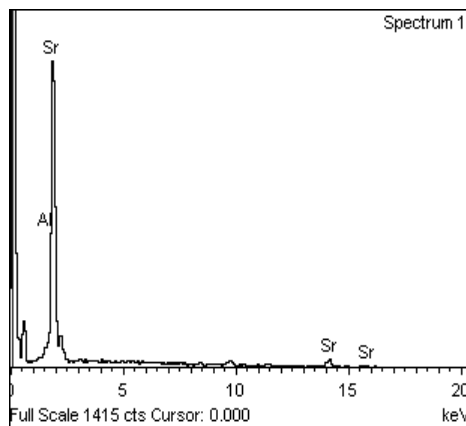


Figure 4. EDS spectra of (a) SrAlO (b) SrAlO:Dy and (c) SrAlO:Mn

The compositional analysis of the samples were determined by EDS is shown in Figure 4 (a-c). The EDS spectrum illustrates peaks linked only to strontium, Aluminum and oxygen like devoid of any impurity peak which verify

that produced nanoparticles are made up of strontium, Aluminum and oxygen.

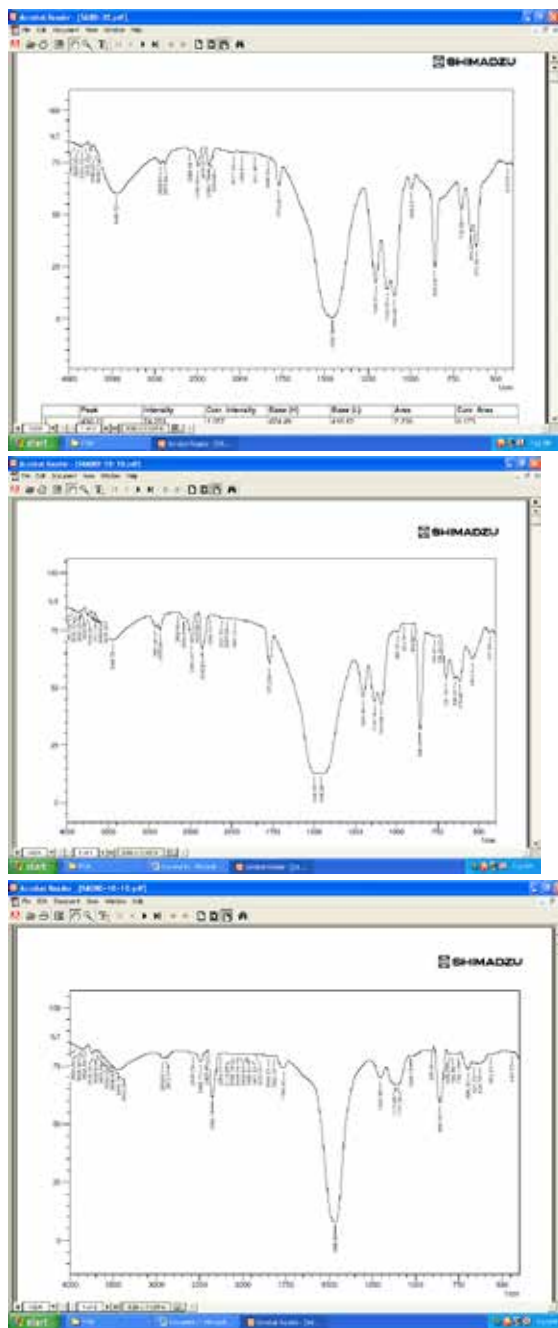


Figure 5. FTIR spectra of (a) SrAlO (b) SrAlO:Dy and (c) SrAlO:Mn

The FT-IR spectra of SrAlO and SrAlO:Mn, Dy are shown in Fig. 5(a-c). The prominent peaks are observed at 3448, 1445, 1027, 857 and 700-400 cm^{-1} due to the presence of adsorbed moisture and M-O bonding respectively. The distinguishable and repeatable peak 3448 cm^{-1} is assigned to the stretching vibration of O-H. Moreover the stretching vibration of O-H could be attributed to the moisture adsorbed surface. FT-IR exhibited absorption bands at 3343 cm^{-1} , 1600 cm^{-1} , and 1400 cm^{-1} accountable for water and CO_2 which usually nanocrystalline materials take up from the environment due to its high surface-to-volume ratio[22-24].

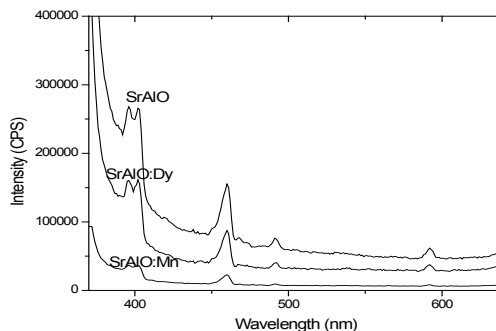


Figure 6. Emission spectra of (a) SrAlO (b) SrAlO:Dy and (c) SrAlO:Mn

The photoluminescence emission spectrum of SrAlO and SrAlO:Mn,Dy is shown in fig. 6(a-c). which is obtained under the excitation wavelength 360nm. The spectra consist of four emission bands: a emission band at ~396 and 402 nm, a blue band at ~460 nm, a weak blue-green band at ~ 485 nm and a very weak yellow at ~590 for SrAlO, SrAlO:Dy and SrAlO:Mn nanoparticles. The strong UV emission corresponds to the exciton recombination related near-band edge emission of nanoparticles. The weak blue and weak blue-green emissions are possibly due to surface defects in the nanoparticles. The weak green band emission corresponds to the singly ionized oxygen vacancy in SrAlO and SrAlO:Mn,Dy. The low intensity of the green emission may be due to the low density of oxygen vacancies during the preparation of the nanoparticles, where as the strong room-temperature UV emission intensity should be attributed to the high purity with perfect crystallinity of the synthesized nanoparticles. It is well known that Dy doped strontium aluminates phosphors show long phosphorescence in green region. But in our case both samples doped or undoped give green emission peak at 480nm with 360nm excitation. The fact that the emission characteristics are excitation dependent shows the emission mechanism is governed mainly by defect controlled processes. Further the emission does not arise from the activator or co-activator ions (as seen in the undoped sample) suggesting that the defect centers act as trap levels in bringing out various emission features. To explain the decrease in photoluminescence intensity, we suggest that incorporation of Dy and Mn ions reduce the defects (exciton, oxygen vacancies), which act as sensitizers for energy transfer due to strong mixing of charge transfer.

Conclusion

In the present work, the SrAlO and Mn, Dy doped SrAlO phosphor were prepared by the Sol Gels method. The XRD study confirms the structure of the system as monoclinic and single phase was obtained due to the calcination temperature. The calculated average crystallite size using Williamson-Hall equation is ~50-90nm. Room-temperature photoluminescence spectra of all the samples showed four main emission bands including a strong UV emission band, a weak blue band, a weak blue-green band, and a weak green band which indicated their high structural and optical quality. Since all the samples are in same crystalline phase, no effective change in the PL properties irrespective of whether the phosphor is doped with Mn and Dy or it is undoped.

REFERENCE

1. F.C. Pallila, A.K. Levine, M.R. Tomkus, J. Electrochem. Soc. 115 (1968) 642. | 2. G. Blasse, W.L. Wanmaker, A. Bril, Philips Res. Repts. 23 (1968)201. | 3. S. Tanabe, J. Kang, T. Hanada, N. Soga, J. Non-Cryst. Solids, 170, (1998)239,. | 4. Z. Aiyu, Y. Ping, C. Yongqiang, Z. Yuanna, Z. Adv. Mat. Lett. 2(5), (2011)322. | 5. A.N. Yerpude, S.J. Dhoble, J. Lumin,132, (2012)1781. | 6. T. Katsumata K. Sasajima, T. Nabae, S. Komuro and T. Morikawa, Journal of Amer. Ceram. Soc., 81, (1998)413. | 7. H. Aizawa, T. Katsumata, J. Takahashi, K. Matsunaga, S. Komuro, T. Morikawa, W. Lehmann, J. Lumin. 5, (1972)87. | 8. R N Bhargava, J. Lumin. 70, (1996)85. | 9. Hanzhuo Jiang, Li Zhang, Yudai Huang, Dianzeng Jia, Zaiping Guo, Materials Science and Engineering B 145 (2007)23. | 10. B. Smets, J. Rutten G. Hoeks, J. Verlijsdonk, J. Electrochem. Soc. 136 (1989) 2119. | 11. T. Matsuzawa, Y. Aoki, N. Takeuchi, Y. Murayama, J. Electrochem. Soc. 143, (1996) 2670. | 12. B.M.J. Smets, Mater. Chem. Phys. 16 (1978) 283. | 13. E. Nakazawa, T. Mochida, J. Lumin. 72-74 (1997) 236. | 14. N.A. Sirazhiddinov, P.A. Arifov, Zhurnal Neorganicheskoi Khimii 16 (1971) 76. | 15. Z. Tang, F. Zhang, Z. Zhang, C. Huang, Y. Lin, J. Eur. Ceram. Soc. 20 (2000) 2129. | 16. A. Nag, and T.R.N. Kutty, J. Alloys. Compd. 354, (2003) 221. | 17. X. Lu, W. Shu, Q. Yu, Q. Fang, and X. Xiong, Glass Phys. Chem. 33, (2007) 62 | 18. S.D. Han, K.C. Singh, T.Y. Cho, H.S. Lee, D. Jakhar, J.P. Hulme, C.H. Han, J.D. Kim, I.S. Chun, and J. Gwak, J. Lumin. 128, (2008) 301. | 19. Z.Y. He, X.J. Wang, W.M. Yen, J. Lumin. 119/120 (2006) 309. | 20. Y.H. Lin, Z.L. Tang, Z.T. Zhang, Mater. Lett. 51 (2001) 14. | 21. S.B. Khan, M. Faisal, M.M. Rahman, A. Jamal, Sci. Tot. Environ. 409 (2011) 2987. | 22. F. Niu, D. Zhang, L. Shi, X. He, H. Li, H. Mai, T. Yan, Mater. Lett. 63 (2009) 2132. | 23. M. Palard, J. Balencie, A. Maguer, J.F. Hochepeid, Mater. Chem. Phys. 20 (2010) 79. |